

FIG. 5. The long wavelength behavior of all approximations considered in this work.

band structure significantly alters the plasmon dispersion for Cs, while its effect is negligible for Na. The plasmon frequency at $q \rightarrow 0$ shows a 0.5 eV renormalization compared to the RPA value within the jellium model. The effect of the band structure in Cs is significantly large enough to dominate over the changes from one kernel to another.

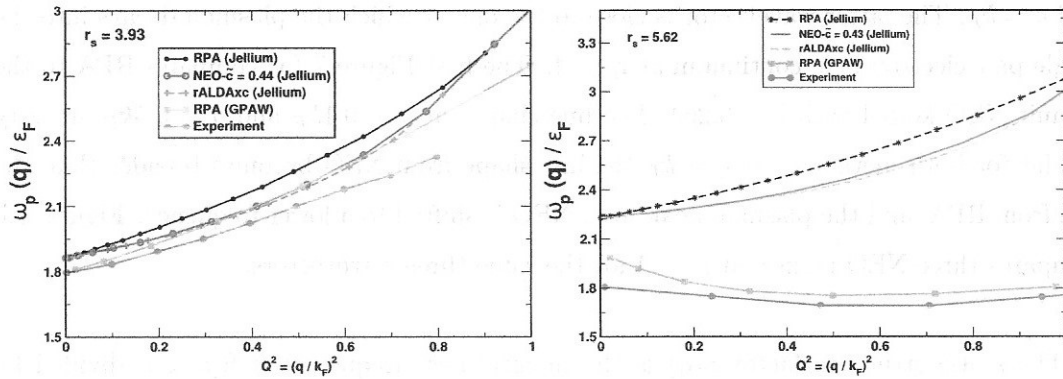


FIG. 6. The plasmon dispersion of Na (left) and Cs (right) with RPA and some exchange-correlation kernels within the jellium model. For Cs, the dispersion with RPA is also displayed with band-structure effects obtained from the GPAW code, showing results close to experiment [7] (also shown). *q is in the (100) direction*

IV. THE DYNAMIC STRUCTURE FACTOR WITHIN AND BEYOND-RPA

The dynamic structure factor [19] or spectral function $S(q, \omega)$ shows the distribution of frequencies ω for density fluctuations of wavevector q in the ground state of the uniform electron gas. Although it arises from all density fluctuations of a given wavevector, the spectral function for small wavevector typically peaks around the frequency of a plasmon. The inverse frequency width of this peak, by the uncertainty principle, provides a lower bound on the decay time for such a fluctuation, while the dependence of the peak on q reflects the plasmon dispersion. Here we will investigate the effects of various model exchange-correlation kernels on the spectral function. The dynamic structure factor $S(q, \omega)$ is proportional to $\text{Im}\chi$ [43], the loss component of the dynamic density-density response function:

$$S(q, \omega) = -\frac{1}{\pi} \text{Im}\chi(q, \omega) \Theta(\omega) \quad \text{not hold faced} \quad (8)$$

This quantity has been investigated by Lewis and Berkelbach [44] using an equation-of-motion coupled cluster singles and doubles formalism, which unlike our TDDFT methods allows for plasmon decay via multi-pair electron-hole decay channels. With our real static exchange-correlation kernels, the plasmon at small finite q does not decay.

In Figure 7, we analyze our approximations at three wavevectors: $q = 0.1k_F$, $q = 0.5k_F$, and $q = k_F$. The latter wavevector is close to the one at which the plasmon decays into the single-pair electron-hole continuum at $r_s = 4$. The first Figure 7 (a) compares RPA to the default NEO kernel with $\tilde{c} = 0.264$. The line shapes at $q = 0.1k_F$ and $q = 0.5k_F$ are very similar for both methods. At $q = k_F$ the line shape from NEO becomes broader than the one from RPA, and the plasmon peak from NEO is shifted to a lower frequency. Figure 7.b compares three NEO kernels at $r_s = 4$ for the same three wavevectors.

The static structure factor $S(q)$ is the integral over frequency of $S(q, \omega)$, divided by the electron number N . $S(q)$ determines the well-known correlation energy of the uniform electron gas. We will now show that the range of q/k_F (less than or about equal to 2) that distributes to the correlation energy is much greater than the range of q/k_F (less than or about equal to 1) that contributes to the plasmon dispersion. In the smaller range (but not in the larger one), the ALDxc kernel is nearly sufficient, while the default NEO kernel is nearly sufficient over the larger range. This completes our plasmon dispersion analysis with

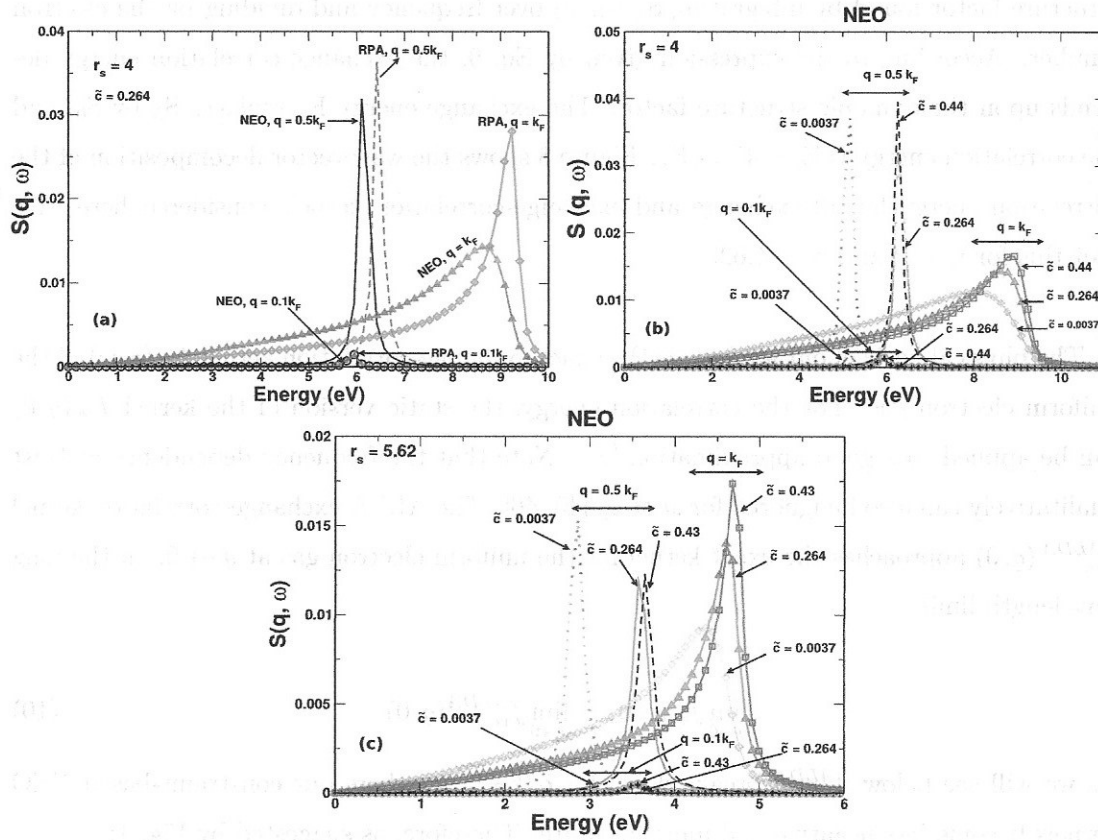


FIG. 7. a: The jellium spectral functions for RPA and NEO $\tilde{c} = 0.264$ at $r_s = 4$. b: the spectral functions for three NEO kernels at $r_s = 4$. c: the jellium spectral functions for three NEO kernels at $r_s = 5.62$ corresponding to Cs.

an explanation why a negative dispersion cannot exist in jellium at the density of Cs.

Exchange-correlation kernels can be applied to improve the ground state correlation energy of RPA through the adiabatic connection fluctuation dissipation theorem. This is the basis of the wavevector decomposition of the ground state exchange-correlation energy as known from Langreth and Perdew [19]:

$$E_{xc} = \int \frac{d^3q}{(2\pi)^3} \frac{1}{2} \int_0^1 \frac{d\lambda}{\lambda} \left(\frac{4\pi\lambda}{q^2} \right) N[S_\lambda(\mathbf{q}) - 1], \quad (9)$$

where λ is the coupling constant along the adiabatic connection path and $S_\lambda(\mathbf{q})$ is the static

not bold-faced

energy. The dynamic structure factor becomes a link that couples the physics in the correlation energy and plasmon dispersion. From the correlation energy, the exact uniform-electron gas-based kernel must be less negative than the ALDAxc kernel. The NEO $\tilde{c} = 0.264$ kernel is uniform electron gas-based only through its energy optimization to the high-density limit, and performs reasonably for both plasmon dispersion and correlation energy in jellium.

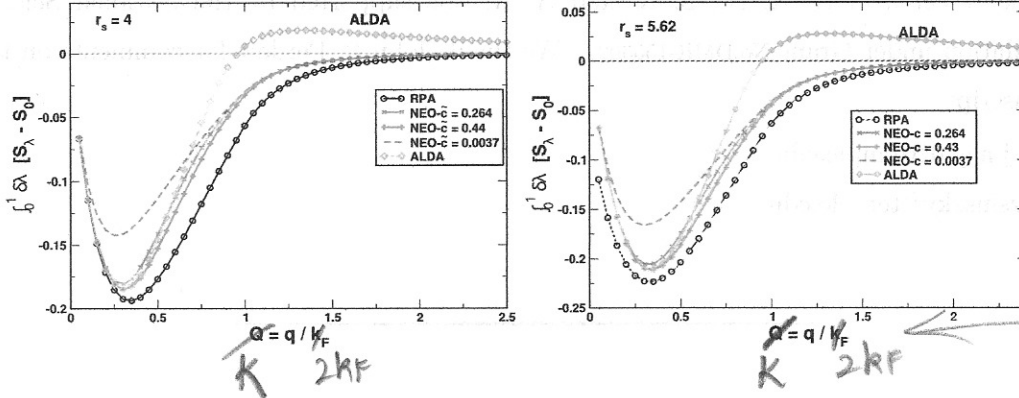


FIG. 8. Wavevector analysis of the ground state correlation-only energy of jellium from the dynamic structure factor for reduced wavevector $Q = \frac{q}{k_F}$. The area under each curve is proportional to the correlation energy. The left figure shows the correlation-only energy for RPA, ALDA and NEO with the three choices for \tilde{c} , for $r_s=4$. The right figure shows the same for $r_s=5.62$ corresponding to Cs.

V. CONCLUSION

We have presented various model exchange-correlation kernels beyond-RPA for the plasmon dispersion within the jellium model for alkali metals. We have shown that the plasmon dispersion is strictly controlled by exact constraints. Additional physics beyond the ALDA kernel, such as nonlocality in space, can be unimportant for plasmon dispersion. In change, physical constraints such as the compressibility sum rule determine the plasmon dispersion with exchange-correlation kernels. Clearly none of our methods based on particle-hole RPA for jellium is able to predict the experimentally observed negative plasmon dispersion for the heavy alkali metal Cs which arises from bandstructure. The current exchange-correlation kernels do not have an explicit density dependence that could have a larger impact. For the exact exchange-correlation kernel, the ALDAxc is likely a lower bound (as suggested by Fig. 1). The ALDAxc is accurate for $\frac{q}{k_F} < 1$, the range of q that determines the plasmon